

# FACULTY OF SCIENCE



Cover photo taken by SeaWiFS Project, NASA, on March 28 2003 [1].

Acknowledgments

Thank you...

#### Abstract

Abstract...

# **Contents**

| l | Intr | oduction                                       | 1  |
|---|------|--|----|
| 2 | The  | ory  | 1  |
|   | 2.1  | The physics behind anticyclones                | 1  |
|   | 2.2  | The physics behind PM 2.5                      | 2  |
|   | 2.3  | The Mann-Kendall test                          | 2  |
| 3 | Met  | hod  | 3  |
|   | 3.1  | The data handling                              | 3  |
|   | 3.2  | The meteorological measuring devices           | 5  |
| 4 | Resi | ult  | 6  |
|   | 4.1  | The evolution of PM 2.5 over time              | 6  |
|   | 4.2  | The frequency of high pressure blocking events | 11 |
| 5 | Disc | eussion  | 13 |
| 6 | Con  | clusion  | 13 |
| 7 | Out  | look   | 13 |

Fredrik Bergely 2 THEORY

## 1 Introduction

It is common knowledge that Earth's increasing temperature has many side effects. One such effect is the increase in frequency of extreme weather phenomena [2]. One such phenomenon, which lacks extensive research, is high-pressure blocking events. High-pressure blocking events is an anticyclone that covers an area for a prolonged period of time and often blocks other types of weather, hence the name. This results in clearer weather and more extreme temperatures [3]. However, an anticyclone is also associated with lower air movement and wind, causing the air to remain stagnant. This can lead to an accumulation of aerosols such as PM<sub>2.5</sub> in the region [4].

To investigate the relationship between  $PM_{2.5}$  and high-pressure blocking, one must analyse periods of high-pressure blocking and examine the concentration of  $PM_{2.5}$  during these periods. The goal of this thesis is to analyse the concentration of  $PM_{2.5}$  during periods of high-pressure blocking by examining data from the Swedish Meteorological and Hydrological Institute (SMHI) and  $PM_{2.5}$  data from rural (Vavihill, Svalöv Skåne county) and urban (Malmö, Skåne county) areas.

# 2 Theory

#### 2.1 The physics behind anticyclones

Anticyclones are meteorological high-pressure systems in which air sinks toward the ground, creating high pressure [5]. This occurs due to the convergence of air from all directions, which forces the air to move downward. The descending air undergoes adiabatic compression, resulting in an increase in the energy of air molecules, or, in other words, a higher temperature. This rise in energy inhibits cloud formation, as the air molecules are unable to ascend due to the lack of cooling. The absence of clouds allows solar radiation to significantly impact the temperature during an anticyclone. Consequently, this leads to a large temperature difference between day and night, with summer anticyclones associated with high temperatures and winter anticyclones with low temperatures. Due to the Coriolis effect, anticyclones rotate in a clockwise direction in the Northern Hemisphere.

#### more on anticyclones

A high-pressure blocking period refers to a prolonged anticyclone characterized by higher surface pressure covering a large area [3]. Since the blocking system extends over a vast region, the pressure gradient remains small due to minimal fluctuations. As a result, winds tend to be calm to gentle breezes. A blocking period is typically defined as lasting between five and ten days, although no single definition exists. While the concept has been recognized in meteorology for over a century, the long-term consequences of blocking events are not yet fully understood. High-

Fredrik Bergely 2 THEORY

pressure blocking periods are more common in the Northern Hemisphere compared to the Southern Hemisphere. Research has indicated that the frequency of blocking periods has increased in recent years [3].

Recurring anticyclones can be classified into Hess and Brezowsky (1977) macrocirculation types, such as the Fennoscandian High (Hfa), the Southeast Anticyclone (Sea), and the Central European High (HM) [6]. These anticyclones are commonly located at specific geographic points. Since anticyclones exhibit winds rotating clockwise around their center, the winds from (Hfa), (Sea), and (HM) tend to blow toward southern Sweden from the south and east. The transport of airborne pollutants, such as ozone, can occur via these winds [7]. Consequently, it can be hypothesized that other airborne aerosols, such as PM<sub>2.5</sub>, should also be transported through these wind patterns.

Moving anticyclones

## 2.2 The physics behind PM 2.5

 $PM_{2.5}$  refers to particulate matter with a diameter of 2.5 µm or less. Although these aerosols can form naturally in the atmosphere, their primary sources include solid fuel combustion for domestic heating, industrial activities, and road transportation [8]. A significant contributor to  $PM_{2.5}$  pollution is the bonding of aerosols to ammonia emitted from agricultural activities. The European Union has set an annual mean limit for  $PM_{2.5}$  concentrations at 25 µg m<sup>-3</sup>. This threshold has been exceeded in several countries, including Croatia, Bosnia and Herzegovina, Italy, Poland, North Macedonia, and Türkiye [?]. Studies have demonstrated a correlation between elevated  $PM_{2.5}$  concentrations and an increased risk of respiratory, cardiovascular, and cerebrovascular diseases, as well as diabetes.

Since PM<sub>2.5</sub> emissions are particularly high in countries such as Poland, anticyclonic winds from (Hfa), (Sea), and (HM) are expected to increase PM<sub>2.5</sub> concentrations in southern Sweden [8]. These aerosols would be transported to southern Sweden via southerly to easterly winds during the anticyclone. If this occurs during a high-pressure blocking event, the aerosols may accumulate over the region while continuously being advected by southerly and easterly winds. Studies in China have shown that the dispersion of aerosols during high-pressure blocking is inhibited [4]. Whether the same occurs in southern Sweden is of interest for further study.

#### 2.3 The Mann-Kendall test

Fredrik Bergely 3 METHOD

## 3 Method

#### 3.1 The data handling

The relevant data was downloaded from the SMHI's website as CSV files. These files included hourly atmospheric pressure data, hourly rain data, and hourly wind data (speed and direction). Hourly PM<sub>2.5</sub> data, measured over one-hour intervals, was also downloaded. Since the goal of this project was to analyse PM<sub>2.5</sub> concentrations in Southern Sweden during high-pressure blocking events, one urban and one rural site were selected. The locations were chosen based on their classification as rural or urban and the length of time the stations had been in operation, where more data was considered better.

The rural measuring station with the most data was Vavihill (Svalöv, Skåne County, Sweden). This station was active from September 28, 1999, to November 15, 2017. However, due to missing data on some days, only 57 % of the period contained non-NaN values. Additionally, between 2017 and 2018, the Vavihill station was relocated to nearby Hallahus, where it operated from May 10, 2018, to December 31, 2022, with 93 % of the period containing non-NaN values. Combining these datasets resulted in a total of 5,371 days of hourly data. For an urban location in Southern Sweden, Malmö had the most data, with measurements recorded from June 3, 1999, to December 31, 2023. Here, 90 % of the recorded values were non-NaN, resulting in 8,074 days of data.

The choice of atmospheric pressure measurement station was Helsingborg, located  $25 \,\mathrm{km}$  from Vavihill and  $49 \,\mathrm{km}$  from Malmö. This location was chosen based on its proximity to both  $PM_{2.5}$  measuring stations, the fact that neither Malmö nor Vavihill have pressure measurements from this period, and the fact that the station has been in use from August 2, 1995, to October 10, 2024, with measurements taken every hour without any missing (NaN) values. This station thus covers the entire period of the  $PM_{2.5}$  data. It is important to note that the measurements are shown as sea-level pressure.

The relevant rain and wind data were gathered from two different stations. For Vavihill, the station at Hörby, located 35 km away, was used, and for Malmö, a weather station just 6 km away was used. The weather station at Hörby was chosen instead of Helsingborg since neither Vavihill nor Hörby are located along the coast, whereas Helsingborg is. The wind and rain data from Hörby were measured from August 1, 1995, to October 1, 2020, with measurements taken every hour without any missing (NaN) values. It is important to note that the Hörby station was temporarily relocated for a short period in 2021. The rain data from Malmö was measured from November 21, 1995, and the wind data from January 1, 1990, with both measurements ending on December 31, 2020. These stations did not lack any data.

To evaluate when there was a high-pressure blocking event for Vavihill or Malmö, the rain data and atmospheric air pressure were used. For a period to be defined as a high-pressure event, the atmospheric pressure had to be over

Fredrik Bergely 3 METHOD

 $1014 \, hPa$ , and the rainfall had to be less than  $0.5 \, mm \, h^{-1}$ . These values were based on the fact that  $1014 \, hPa$  was the mean atmospheric pressure from Helsingborg, and  $0.5 \, mm \, h^{-1}$  was chosen since this is considered light rain. For a high-pressure event to be considered a high-pressure blocking event, the criteria for a high-pressure event had to persist for at least  $120 \, h$  (5 days). This value was chosen since a 5-day limit is often considered when classifying high-pressure blocking events.

The data was analysed by taking the mean and standard deviation of each hour of the high-pressure blocking event, from hour one, to evaluate the average progression of a blocking over time using the Python packages NumPy and pandas. Since the blocking events varied in length, the number of data points was also plotted, with the requirement that each hour consist of at least 8 data points. This resulted in a plot of the mean concentration of  $PM_{2.5}$  for every hour from the beginning of the blocking period, for both Vavihill and Malmö. All of the  $PM_{2.5}$  plots were evaluated together with the mean value when there was no blocking and the EU annual mean limit for  $PM_{2.5}$ . Due to the lack of  $PM_{2.5}$  data during some periods, a filter was applied, stating that a period needed 95 %  $PM_{2.5}$  coverage in order to be analysed.

Afterwards, the data was sorted in different ways to explore how the  $PM_{2.5}$  concentration depended on different parameters. Firstly, the data was sorted into one of four wind categories: North-East (310° to 70°), South-East (70° to 190°), West (190° to 310°), and no specific direction. This was done by categorizing the data if 60 % of the wind directional data fell into one of these categories, with no wind being handled as a NaN value.

Secondly, the data was sorted based on the season of the blocking. This was evaluated by taking the midpoint date of the blocking and categorizing the season by the month it occupied. December, January, and February were considered winter; June, July, and August were considered summer; and spring and autumn were the remaining months. Lastly, the data was categorized based on the strength of the high-pressure blocking, where a weak high-pressure blocking event had a mean atmospheric pressure between 1014 hPa and 1020 hPa, a medium-strength blocking event had a mean atmospheric pressure between 1020 hPa and 1025 hPa, and a strong blocking event had a mean atmospheric pressure over 1025 hPa.

To evaluate if the plots produced significant results, two tests were performed. The first test compared the mean and standard deviation of  $PM_{2.5}$  during high-pressure blocking events with the mean and standard deviation during periods without high-pressure blocking. Secondly, the Mann-Kendall test was performed to evaluate whether the  $PM_{2.5}$  mean during high-pressure blocking events had actually increased, and if so, by how much. This was done by assessing whether the p-value was below 0.05 and whether  $\tau$  was above 0.5.

The second task was to evaluate whether high-pressure blocking events had become increasingly more common. This was evaluated in two different ways: by calculating the number of high-pressure blocking events per year, and the number and lengths of high-pressure blocking events per year. The number of days of blocking was also sorted by the season of the blocking to provide more insight into the nature of the high-pressure blocking events. For

Fredrik Bergely 3 METHOD

this evaluation, atmospheric pressure data from Ängelholm was used instead of Helsingborg due to the pressure data from Ängelholm being active from January 5, 1946, to October 1, 2024, meaning it has been in service for 49 years longer than that from Helsingborg. This station is located 44 km from Vavihill and 76 km from Malmö. However, the pressure values differed only by a mean of 0.25 hPa and a standard deviation of 0.20 hPa. The rain data was also expanded by using daily rain data from Ängelholm since this data was gathered from January 18, 1947, to November 30, 2001. To obtain the maximum amount of the the rain data the data from Ängelholm was used together with the nearby station of Tånga. This station is located 12 km away and had been in use between December 19, 1973, to August 31, 2024.

#### 3.2 The meteorological measuring devices

The wind data from both Hörby and Helsingborg used the high-performance wind sensor Vaisala WAA15A for the wind speed and Vaisala WAV15A for the wind direction. These instruments were serviced and calibrated every year or every other year, and had been in use since 1995. The WAA15A anemometer measured wind speed with an accuracy of 0.17 m s<sup>-1</sup>, and the WAV15A wind vane measured the wind direction with an accuracy better than 3°[9]. The WAA15A anemometer works by a rotating chopper disc that interrupts an infrared beam, resulting in a laser pulse proportional to the wind speed. The WAV15A wind vane uses a counterbalanced vane with an optical disc. When the vane turns, infrared LEDs detect the change in angle with the disc and phototransistors, resulting in a precise measurement of the wind angle. For rain monitoring, the Geonor T200 device had been in use for all stations since 1995. Like the wind monitor, this device had been serviced and calibrated every year or every other year. This device works by measuring precipitation with a vibrating wire sensor that detects weight changes from the water droplets[10]. The device has a measurement accuracy better than 0.1 mm.

The barometer that has been in use for Helsingborg is a Vaisala PTB201A for the entire period, except for the periods from April 15, 2015, to April 17, 2025, and from September 19, 2004, to May 23, 2014, when a Vaisala PTB220 was used instead. Even then, the device has been serviced every year or every other year. The PTB201A digital barometer operates using a silicon capacitive absolute pressure sensor, providing stable and accurate pressure values [11]. The sensor functions by means of a flexed diaphragm inside a capacitor that bends in response to air pressure, causing a change in the capacitor's distance and thus a variation in the current. This device measures pressure in the range of 600 hPa to 1100 hPa, with an accuracy of 0.3 hPa. Errors in the device may arise due to environmental factors, such as exposure to condensing gases. The Vaisala PTB220 digital barometer operates in a similar manner but offers a wider measurement range of 500 hPa to 1100 hPa, with an improved accuracy of 0.15 hPa [12].

- How was wind and rain in Malmö measured?
- How was pressure in Ängelholm and rain in Ängelholm/Tånga measured?
- What PM2.5 measurement devices was used in Vavihill/ Malmö?

#### 4 Result

#### 4.1 The evolution of PM 2.5 over time

After applying the high-pressure blocking detection method to the data from Vavihill for the entire period, a total of 298 high-pressure blocking events were identified between August 1, 1995, and October 10, 2024. Of these 298 events, 171 were removed due to insufficient PM<sub>2.5</sub> data, as a filter requiring 95% data coverage was applied. This left 127 relevant high-pressure blocking events. For Malmö, a total of 299 high-pressure blocking events were identified between November 20, 1995, and October 1, 2024. From these, 99 events were removed due to insufficient PM<sub>2.5</sub> data, again applying the 95% data coverage filter. This resulted in 200 relevant high-pressure blocking events. An example plot showing the periods of high-pressure blocking events can be seen in Figure 1.

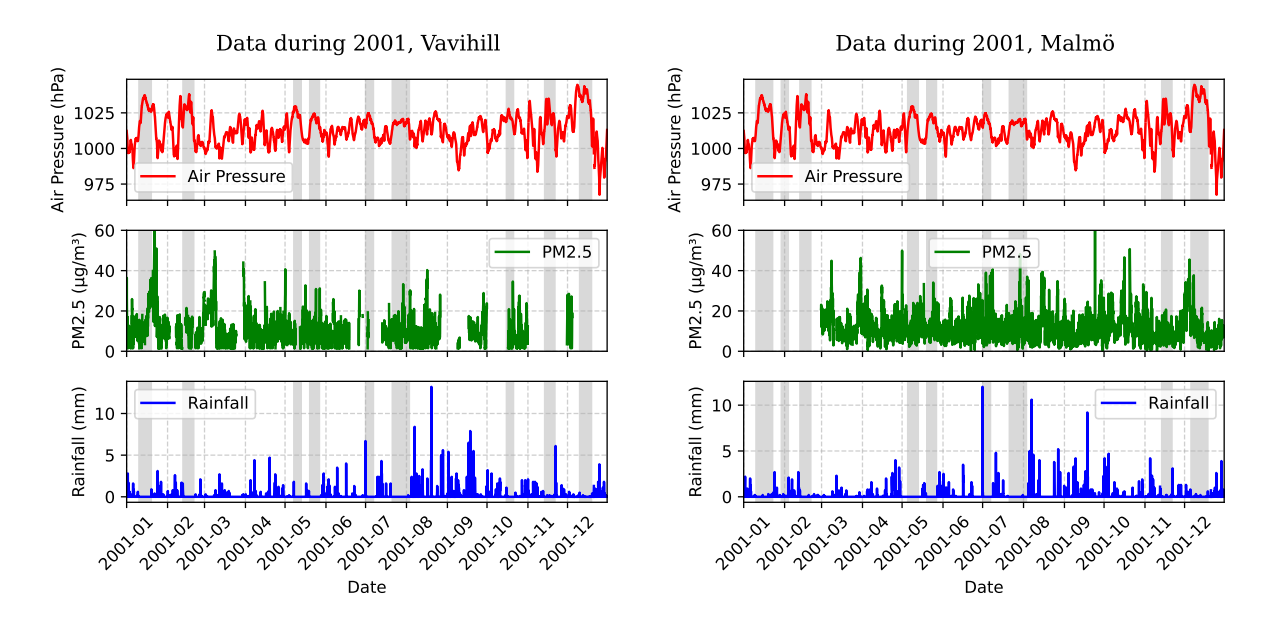
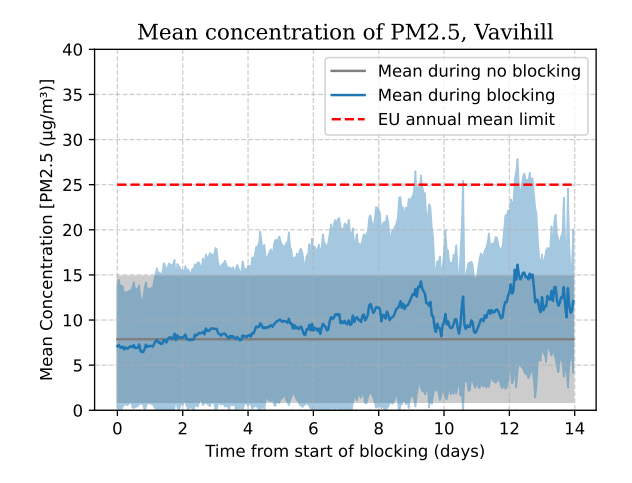
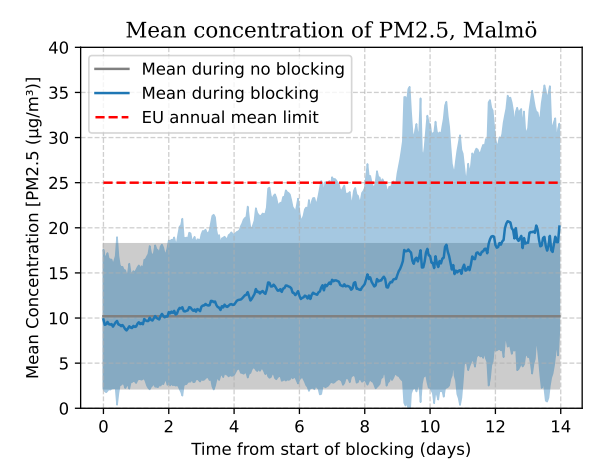


Figure 1: These example plot displays the air pressure,  $PM_{2.5}$  concentrations, and rainfall during the year 2001. The periods which was indicated as periods of high-pressure blocking events are shown in gray.

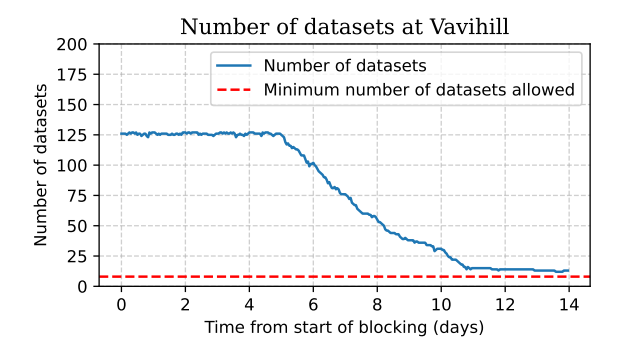
The second task was to evaluate the  $PM_{2.5}$  concentrations during periods of high-pressure blocking by taking the mean concentration from the start of the event. This can be seen in Figure 2. The data is compared with the  $PM_{2.5}$  mean taken from periods without high-pressure blocking events. An increase in  $PM_{2.5}$  concentrations can be seen in Malmö, while a slight increase can be observed in Vavihill. It is important to note that after the first five days, the number of datasets decreases, which is reflected in the increase in standard deviation.

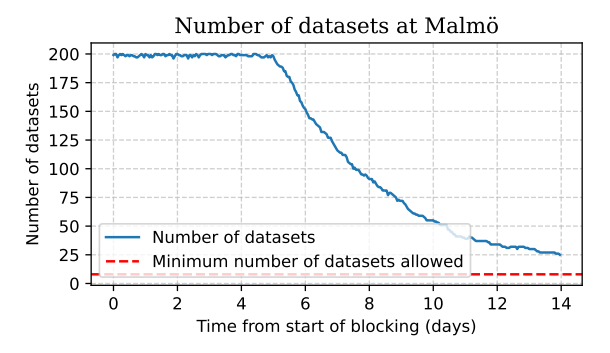




(a) This figure shows the mean PM<sub>2.5</sub> concentrations over time in Vavihill. The data is analysed to observe trends and variations in air pollution levels in a rural setting.

(b) This figure shows the mean  $PM_{2.5}$  concentrations over time in Malmö. The data is analysed to observe trends and variations in air pollution levels in an urban environment.



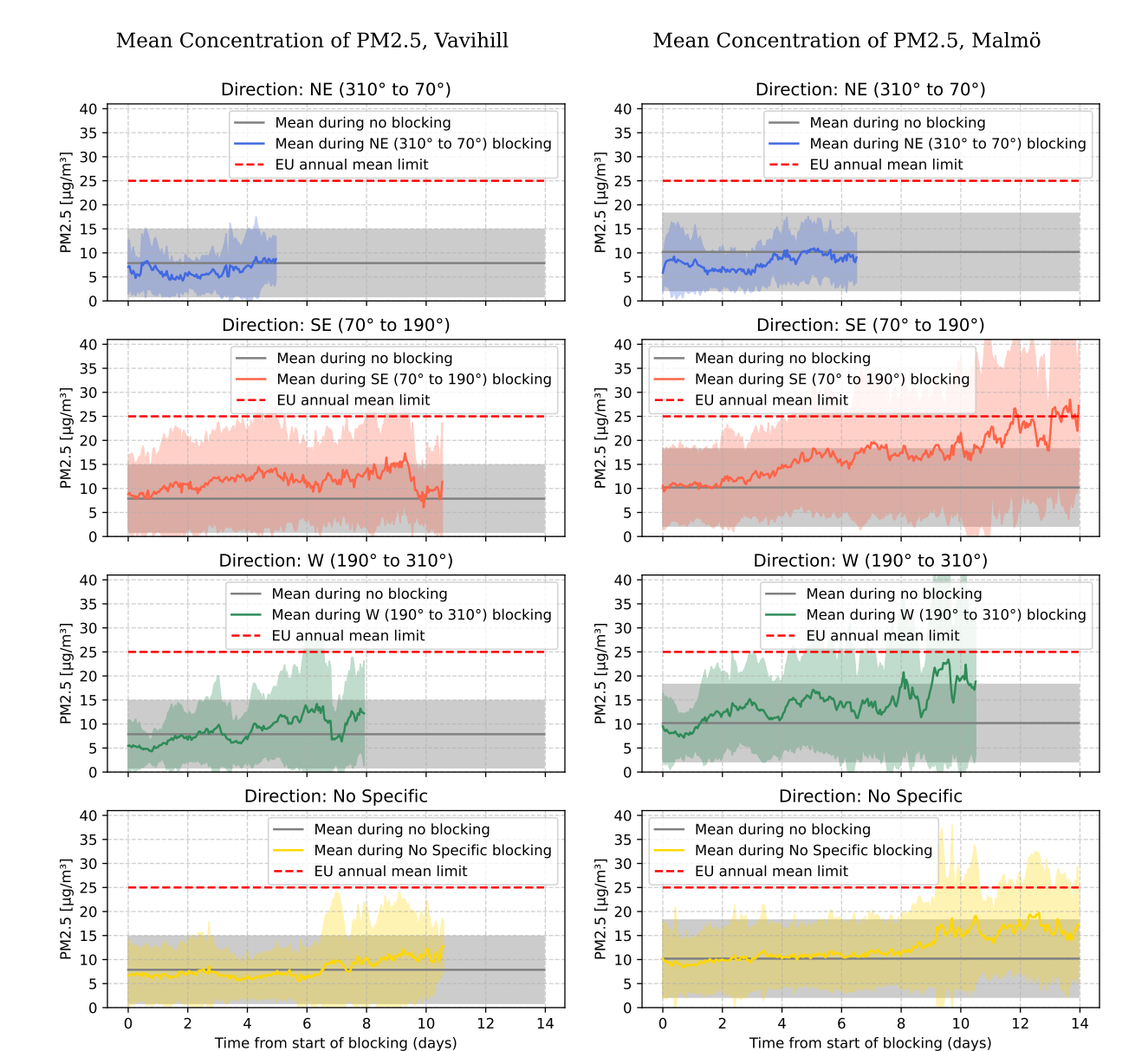


(c) This plot shows the number of datasets used per day for the calculation above at Vavihill.

(d) This plot shows the number of datatsets used per day for the calculation above at Malmö.

Figure 2: Comparison of mean  $PM_{2.5}$  concentrations in Vavihill and Malmö, highlighting differences between rural and urban air quality. The shaded region indicates the standard deviation of the data.

The change in  $PM_{2.5}$  concentrations in Vavihill and Malmö for different wind directions can be seen in Figure 3. One can see similarities between the wind directions for Vavihill and Malmö, although the extremes are more pronounced in Malmö. When the wind filter was applied for the NE direction (310° to 70°), no clear increase or high levels of  $PM_{2.5}$  were detected. The same is true for the non-specific wind direction in Vavihill. For the other directions, an increase in  $PM_{2.5}$  can be seen. Elevated levels can also be seen in Vavihill for the SE direction (70° to 190°), in Malmö for the W direction (190° to 310°), and especially in Vavihill for the SE direction (70° to 190°).



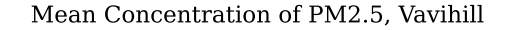
(a) These plots show how  $PM_{2.5}$  concentrations change in Vavihill for different wind directions. It is important to note that 6.3% of the winds came from the Northeast (310° to 70°), 39.9% from the Southeast (70° to 190°), 21.3% from the West (190° to 310°) and 42.5% from no specific direction.

(b) These plots show how  $PM_{2.5}$  concentrations change in Malmö for different wind directions. It is important to note that 7.5% of the winds came from the Northeast (310° to 70°), 24.0% from the Southeast (70° to 190°), 18.5% from the West (190° to 310°) and 50.0% from no specific direction.

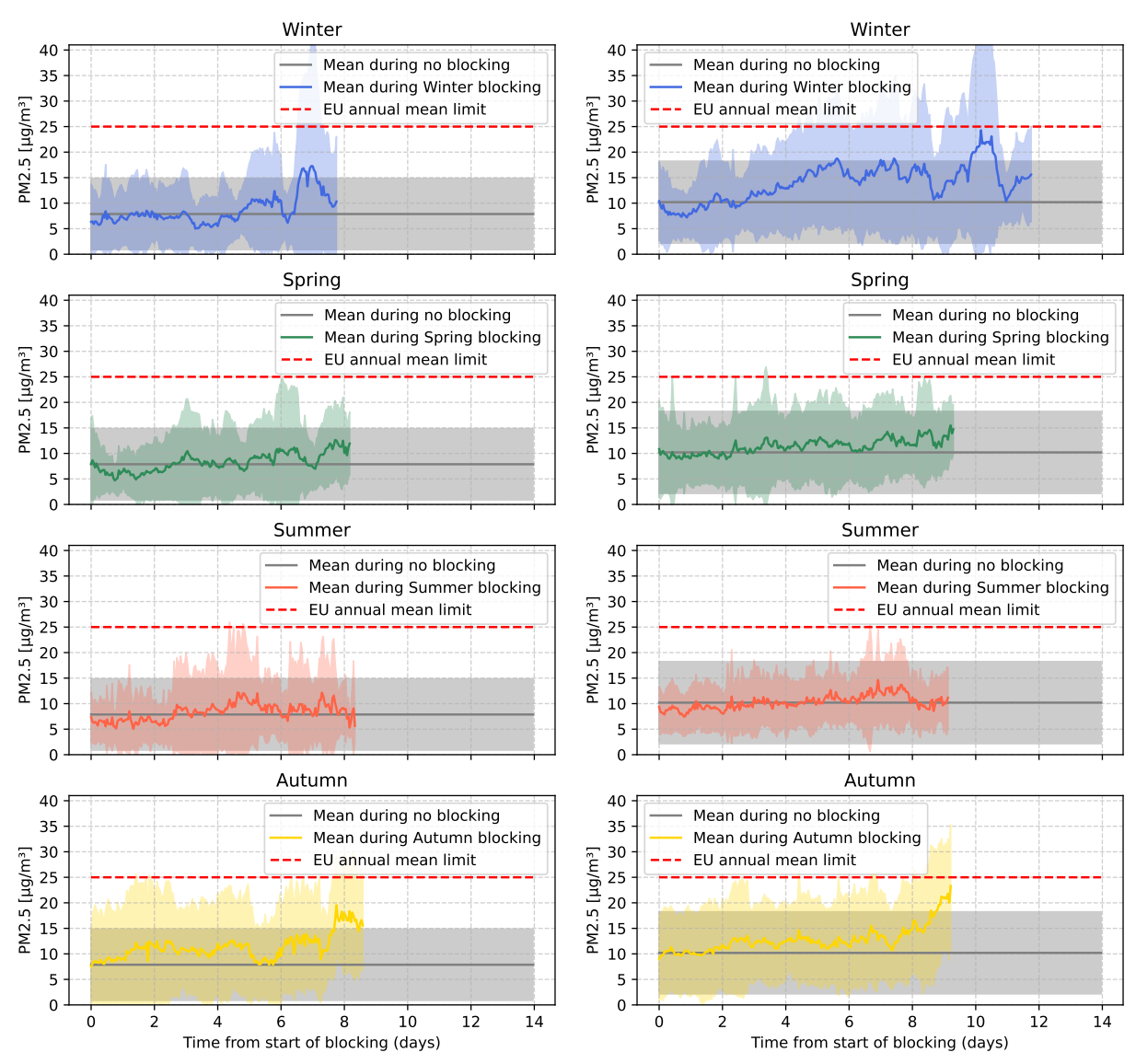
Figure 3: Comparison of  $PM_{2.5}$  concentrations in Vavihill and Malmö for different wind directions. Note that a minimum number of datasets was still put to 8, resulting in some directions having very little data. The shaded region indicates the standard deviation of the data.

How the concentrations of  $PM_{2.5}$  changed due to seasonal variation can be seen in Figure 4. From these plots, it is clear that the concentration during the summer for both Vavihill and Malmö does not indicate an increase nor high levels of  $PM_{2.5}$ . A slight increase can be seen in the case of spring for both locations. A larger increase can be seen during the autumn, where high levels of  $PM_{2.5}$  can be observed towards the end of the period. The winter in Vavihill indicates an increase in the  $PM_{2.5}$  concentrations, although the standard deviation indicates highly dispersed data. Winter in Malmö indicates an increase in  $PM_{2.5}$  concentrations, although the levels seem to lower towards the end

of the period.



#### Mean Concentration of PM2.5, Malmö



(a) These plots show how  $PM_{2.5}$  concentrations change in Vavihill for different seasons. It is important to note that 21.1% of the blocking events occurred during the winter, 27.4% during the spring, 24.2% during the summer and 27.4% during the

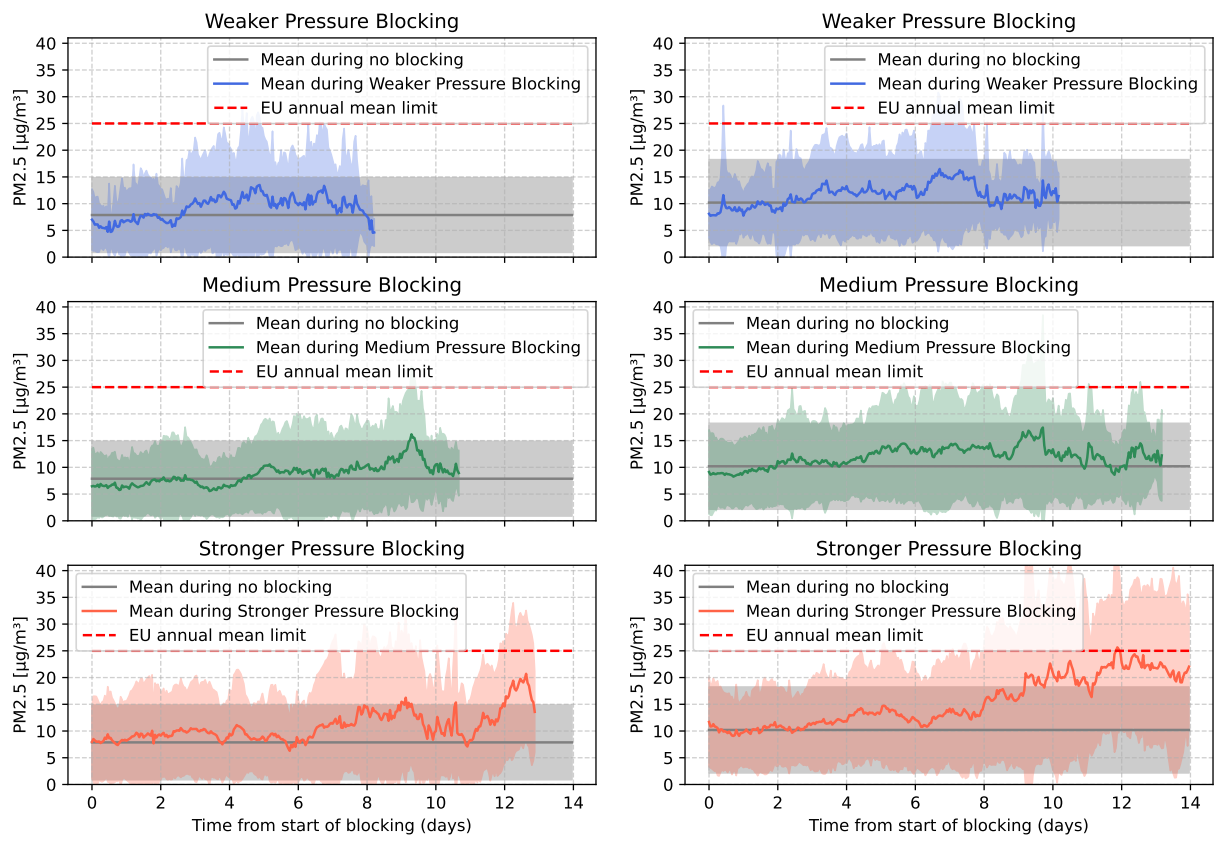
(b) These plots show how  $PM_{2.5}$  concentrations change in Malmö for different seasons. It is important to note that 24.0% of the blocking events occurred during the winter, 34.0% during the spring, 18.0% during the summer and 24.0% during the autumn.

Figure 4: Comparison of  $PM_{2.5}$  concentrations in Vavihill and Malmö for different seasons. Note that a minimum number of datasets was still put to 8. The shaded region indicates the standard deviation of the data.

The increase in  $PM_{2.5}$  concentrations depending on the strength of the high-pressure blocking event can be seen in Figure 5. From the plots, we can observe similar behaviour in the two locations. For weaker and medium-strength high-pressure blocking events, a slight increase in  $PM_{2.5}$  can be seen, although no significantly elevated concentrations are observed. However, in the case of stronger high-pressure blocking events, a more pronounced increase in  $PM_{2.5}$  concentrations can be noticed, along with elevated levels of  $PM_{2.5}$ , especially in Malmö.

#### Mean Concentration of PM2.5. Vavihill

#### Mean Concentration of PM2.5, Malmö



(a) These plots show how  $PM_{2.5}$  concentrations change in Vavihill for different seasons. It is important to note that 20.5% of the blocking events occurred with a mean pressure below 1020 hPa 44.9% occurred between 1020 and 1025 hPa and 34.6% occurred with a mean pressure over 1025hPa.

(b) These plots show how  $PM_{2.5}$  concentrations change in Malmö for different seasons. It is important to note that 17.0% of the blocking events occurred with a mean pressure below 1020 hPa 48.5% occurred between 1020 and 1025 hPa and 34.5% occurred with a mean pressure over 1025hPa.

Figure 5: Comparison of  $PM_{2.5}$  concentrations in Vavihill and Malmö for different strength of the high pressure blocking. Note that a minimum number of datasets was still put to 8.

The result from the Mann-Kendall test can be viewed in Table 1 and Table 2. All of the categories had a p-value approximately equal to 0. The  $\tau$ -value can also be viewed. From this, it is clear that the total mean, the western direction, the spring season, and the pressure strengths medium and strong showed a moderate increase in Vavihill. In the case of Malmö, a moderate increase could be seen during the winter season, as well as in the spring, autumn, and stronger pressure events. Even stronger increases could be seen in the total mean, southeastern direction, and the unspecified direction.

Table 1: Mann-Kendall Test for Vavihill

Table 2: Mann-Kendall Test for Malmö

| Filter     | Category                             | Tau   |
|------------|--------------------------------------|-------|
| Total Mean |                                      | 0.674 |
|            | NE (310° to 70°)                     | 0.353 |
| D!4!       | SE ( $70^{\circ}$ to $190^{\circ}$ ) | 0.461 |
| Direction  | W (190° to 310°)                     | 0.612 |
|            | No Specific Direction                | 0.440 |
|            | Winter                               | 0.449 |
| Coogan     | Spring                               | 0.582 |
| Season     | Summer                               | 0.360 |
|            | Autumn                               | 0.466 |
|            | Weaker                               | 0.399 |
| D          | Medium                               | 0.592 |
| Pressure   | Stronger                             | 0.515 |

| Category              | Tau  |
|-----------------------|--|
|                       | 0.766  |
| NE (310° to 70°)      | 0.368  |
| SE (70° to 190°)      | 0.761  |
| W (190° to 310°)      | 0.581  |
| No Specific Direction | 0.751  |
| Winter                | 0.500  |
| Spring                | 0.605  |
| Summer                | 0.488  |
| Autumn                | 0.623  |
| Weaker                | 0.366  |
| Medium                | 0.307  |
| Stronger              | 0.643  |
|                       | NE (310° to 70°) SE (70° to 190°) W (190° to 310°) No Specific Direction Winter Spring Summer Autumn Weaker Medium |

# 4.2 The frequency of high pressure blocking events

The last task was to determine whether high-pressure blocking events have become more common. Here the 24 hour rain-limt was set to 4 mm, since this corresponds to little rainfall. When looking at the number of high-pressure blocking events per year, no significant change in frequency could be seen (see Figure 6). Since the highest levels of PM<sub>2.5</sub> occurred toward the end of the events (see Figure 2, Figure 3, Figure 4, and Figure 5), the frequency of longer high-pressure blocking events was also examined. However, no distinct increase could be observed in any of the cases.

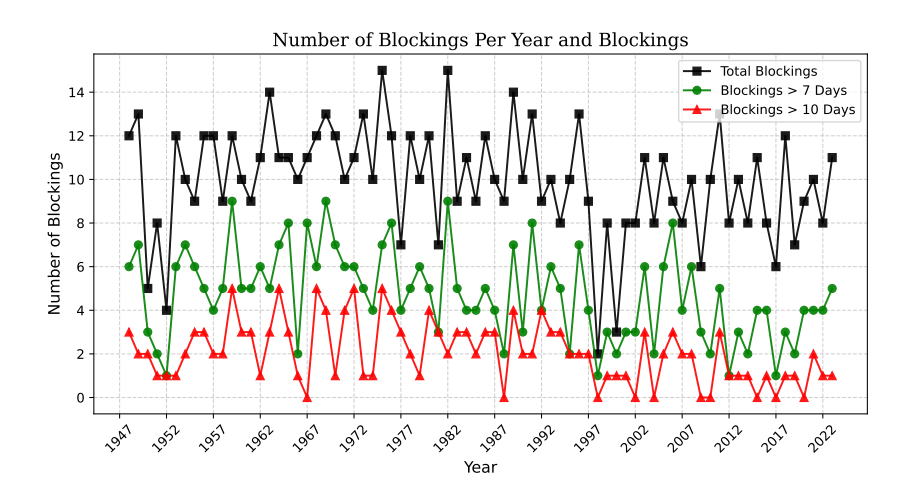


Figure 6: fig: This plots shows the change in frequency of high-pressure blocking events. The plots also indicates the change in events longer than 7 and 10 days.

In Figure 7, the number of days under high-pressure blocking events per year can be seen. Here, the total, seasonal, and pressure strength dependence can be observed. The reason for not including the directional dependence is that this was not available from the data. However, these plots show no clear increase or decrease in the number of days under high-pressure blocking events.

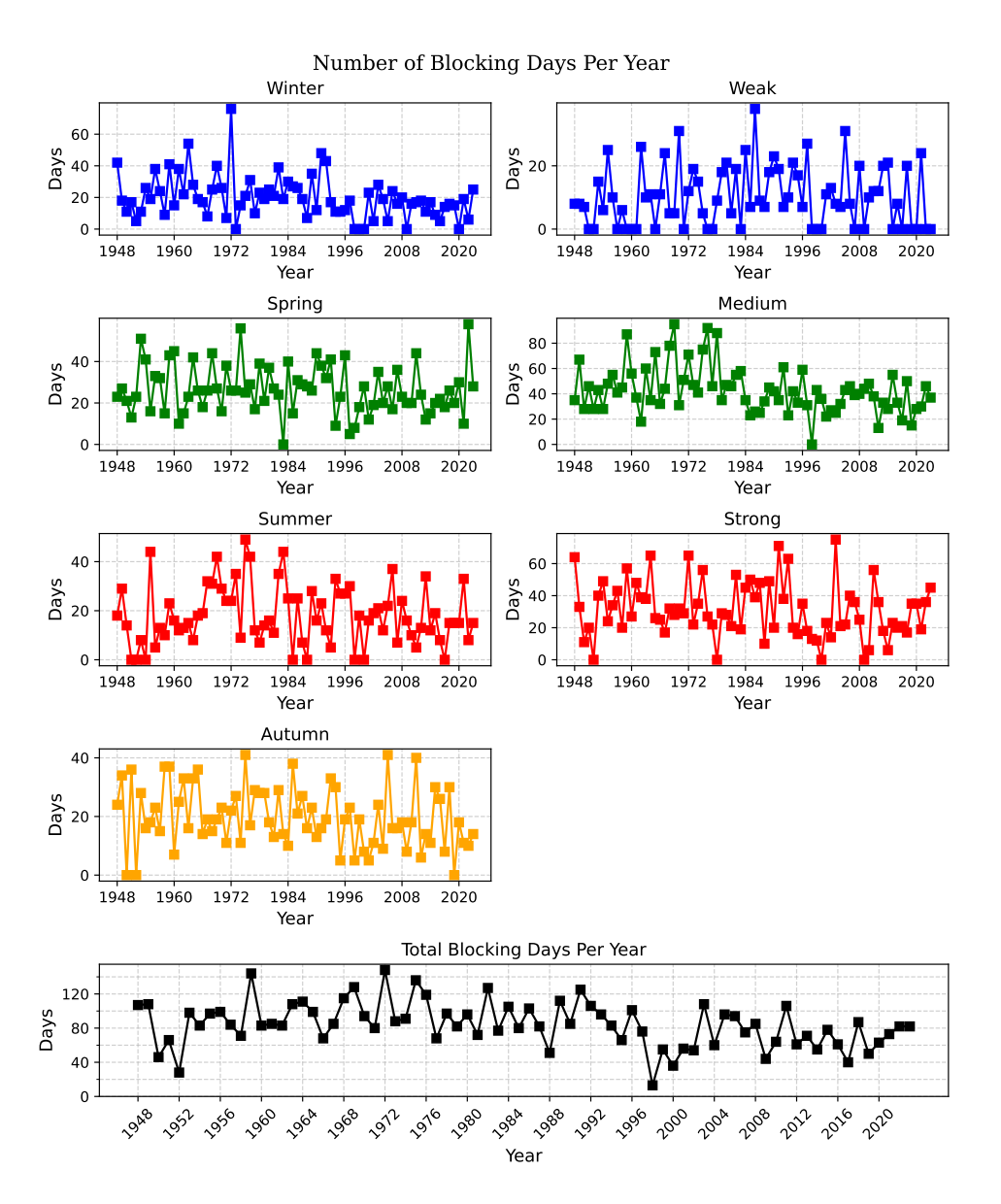


Figure 7: These plots show the change in frequency of days under high-pressure blocking events. The number of days under a high-pressure blocking event each year, during each season, and for different pressure strengths can also be seen.

Fredrik Bergelv 7 OUTLOOK

- 5 Discussion
- 6 Conclusion
- 7 Outlook

Fredrik Bergelv REFERENCES

## References

- [1] NASA. Haze over Europe. https://earthobservatory.nasa.gov/images/11219/haze-over-europe, March 2003.
- [2] John F. B. Mitchell, Jason Lowe, Richard A. Wood, and Michael Vellinga. Extreme events due to human-induced climate change. *Philosophical Transactions of the Royal Society A: Mathematical, Physical and Engineering Sciences*, 364(1845):2117–2133, 2006.
- [3] Anthony R. Lupo. Atmospheric blocking events: A review. https://nyaspubs.onlinelibrary.wiley.com/doi/abs/10.1111/nyas.1455 December 2020.
- [4] Wenyue Cai, Xiangde Xu, Xinghong Cheng, Fengying Wei, Xinfa Qiu, and Wenhui Zhu. Impact of "blocking" structure in the troposphere on the wintertime persistent heavy air pollution in northern China. *Science of The Total Environment*, 741:140325, 2020.
- [5] Vlado Spiridonov and Ćurić Mladjen. Cyclones and Anticyclones | SpringerLink. https://link.springer.com/chapter/10.1007/978-3-030-52655-9\_17, November 2020.
- [6] Judit Bartholy, Rita Pongracz, and Margit Pattantyús-Ábrahám. European Cyclone Track Analysis Based on ECMWF ERA-40 Data Sets. *International Journal of Climatology*, 26(11):1517–1527, 2006.
- [7] Noelia Otero, Oscar E. Jurado, Tim Butler, and Henning W. Rust. The impact of atmospheric blocking on the compounding effect of ozone pollution and temperature: A copula-based approach. *Atmospheric Chemistry and Physics*, 22(3):1905–1919, 2022.
- [8] European Environment Agency. Europe's air quality status 2024. https://www.eea.europa.eu/publications/europes-air-quality-status-2024, 2024.
- [9] VAISALA. Wind Set WA15 and WA25. https://www.vaisala.com/en/products/weather-environmental-sensors/wind-set-wa15, January 2021.
- [10] GEONOR, Inc. T-200B Series All Weather Gauge. https://www.geonor.com/t-200b-all-weather-precipitation—rain-gauge, 2019.
- [11] VAISALA. PTB 200 DIGITAL BAROMETERS USER'S GUIDE, February 1993.
- [12] VAISALA. PTB220 Series Digital Barometers USER'S GUIDE, August 2001.